Supporting information

Au (111)@Ti_6O_{11} heterostructure composite with enhanced synergistic effects as efficient electrocatalyst for hydrogen evolution reaction

Gangquan Xiong [a1], Yanwei Wang [b1], Fan Xu [a], Gangrong Tang [b], Huijuan Zhang [b*], Feipeng Wang [a*], Yu Wang [a,b*]

[a] The School of Electrical Engineering, and State Key Laboratory of Power Transmission Equipment & System Security and New Technology, Chongqing University, 174 Shazheng Street, Shapingba District, Chongqing City, 400044, P. R. China

[b] The School of Chemistry and Chemical Engineering, Chongqing University, 174 Shazheng Street, Shapingba District, Chongqing City, 400044, P. R. China

[1]*the authors contributed equally to this work*

**Corresponding author: E-mail: wangy@cqu.edu.cn (Yu Wang)*

E-mail: zhanghj@cqu.edu.cn (Huijuan Zhang)

E-mail: fpwang@cqu.edu.cn (Feipeng Wang)

Theoretical section

Computation methods

In this work, all the theoretical computations were performed by using the Perdew-Burker-Ernzerhof (PBE) version of the generalized gradient approximation (GGA)[1] within the DFT framework as implemented in Vienna ab initio simulation package (VASP).[2] The project-augmented wave (PAW) method was carried out to represent the interaction between ion and electron,[3] and the cut of energy was set of 400eV.[4] Additionally, the convergence criteria for the ionic forces and the optimization of energy were set to be 0.03 eV/Å and 10^{-5} per atom, respectively. The DFT + U method was employed to treat localized Ti 3d orbitals with an effective U value of 4 eV.[5] Then we selected a 5×3√3 relaxed Au (111) on top of relaxed 1×2 Ti_6O_{11} surface to model Au (111)@Ti_6O_{11} heterostructure.

Calculations of Hydrogen Evolution Reaction

It's acknowledged that the hydrogen evolution reaction (HER) activity over a specific system can be closely bound up with the adsorption energy of a single H atom on the system. The Gibbs free energy of adsorbed state was calculated as:

$$\Delta G(H_*) = \Delta E(H_*) + \Delta ZPE - T\Delta S$$

where ΔE (H*) is the hydrogen chemisorption energy, ΔZPE is the zero point energy difference between adsorbed and the gas phase and TΔS is the entropy change of H*. ΔS was calculated by the formula :

$$\Delta S = S(H_*) - \frac{1}{2}S(H_*) \approx -\frac{1}{2}S(H_*)$$

Where S (H_2) is the entropy of H_2 in the gas phase at standard condition. Considering that TS (H_2) is 0.40 eV for H_2 at 298 K and 1 atm, the corresponding TΔS was determined to be -0.20 eV. Furthermore, the equation $\Delta ZPE = ZPE(H_*) - \frac{1}{2}ZPE(H_2)$ was carried out to assess zero point energy change of H*.

Materials

Titanium dioxide (TiO_2, P25, Fisher Chemical, 99.99%), hydrochloric acid (HCl, 37 wt%, J.T.Baker), sodium hydroxide (NaOH, 99.9%, Aldrich), chloroauric acid ($HAuCl_4 \cdot 4H_2O$, 99%, Aldrich) , and Nafion (5 wt%, Sigma-Aldrich) were of analytical grade and were used without further purification. Deionized (DI) water was supplied with a HuaChuang ultra-pure water system (18.5 MΩ • cm) and was used in the preparation of all solution.

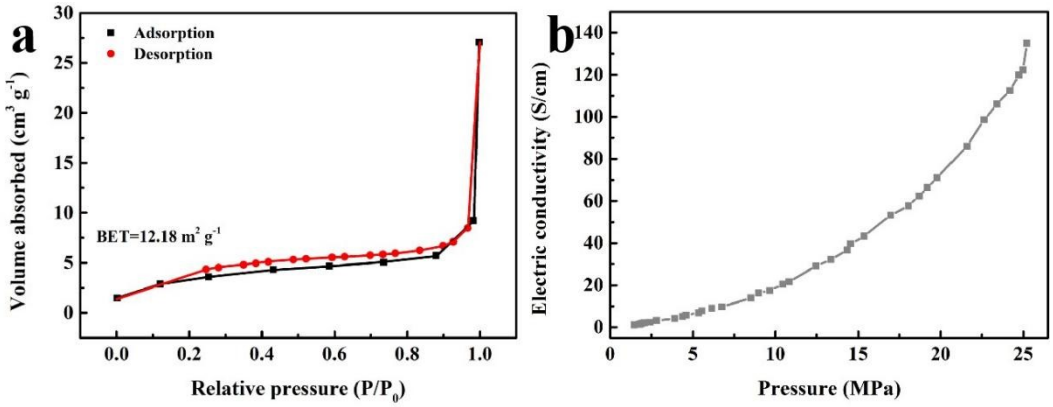

Fig. S1. (a) N_2 Adsorption-desorption isotherms of Ti_6O_{11}; (b) The electric conductivity/pressure curve of Ti_6O_{11}.

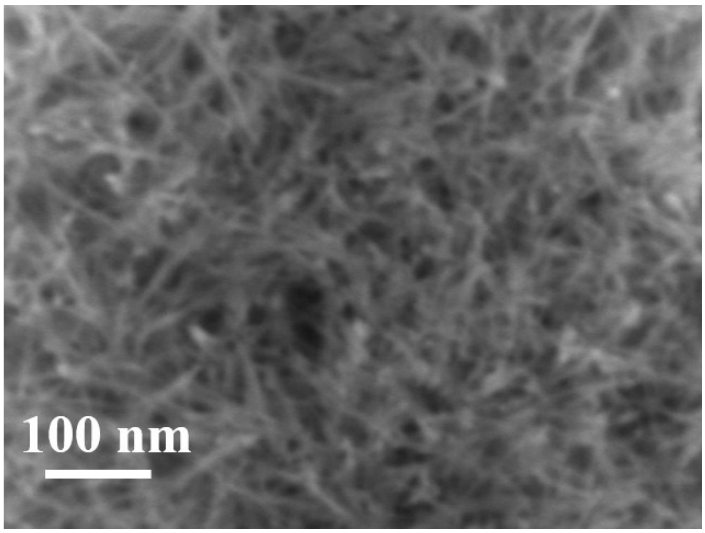

Fig. S2. The SEM image of TiO_2 nanotubes precursor.

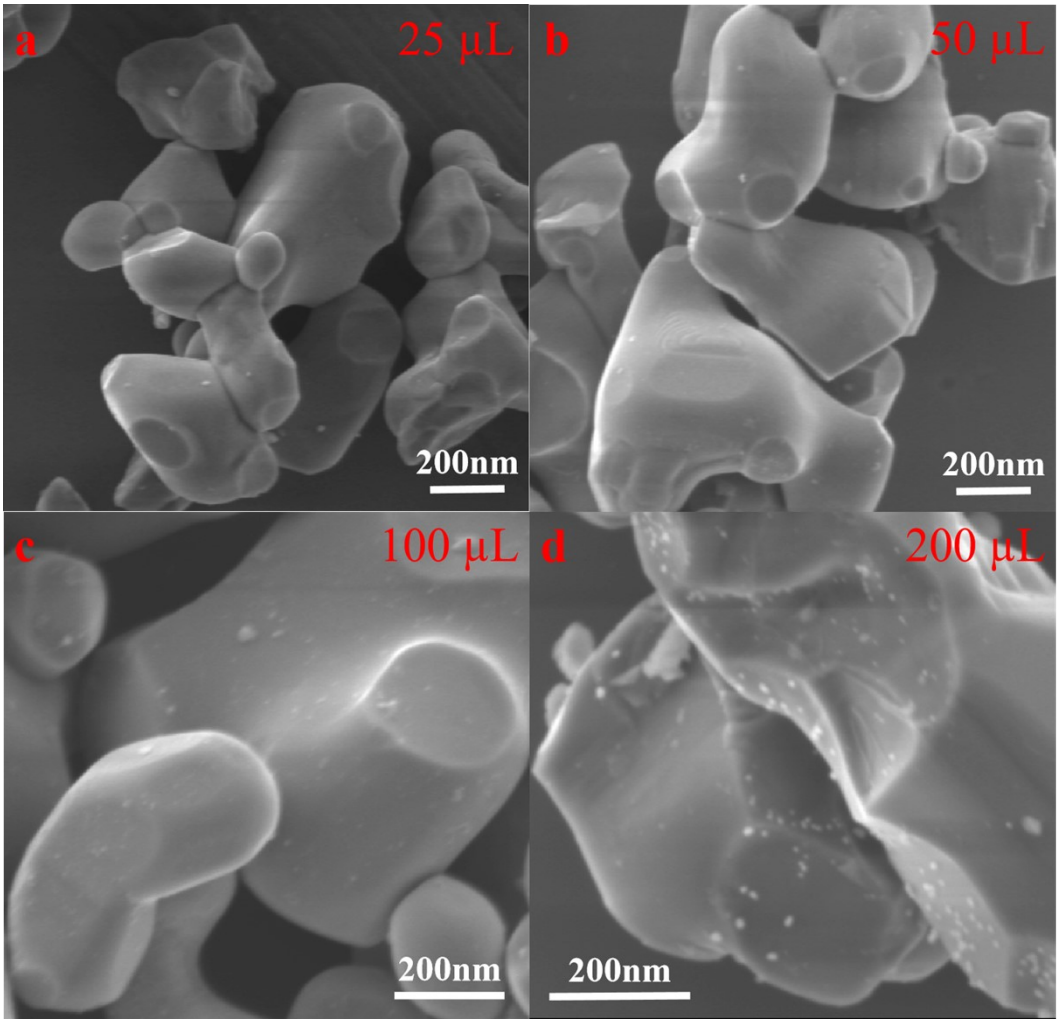

Fig. S3. (a)~(d) The SEM images of Au (111)@Ti_6O_{11}-x, (x=25, 50, 100, 200 μL).

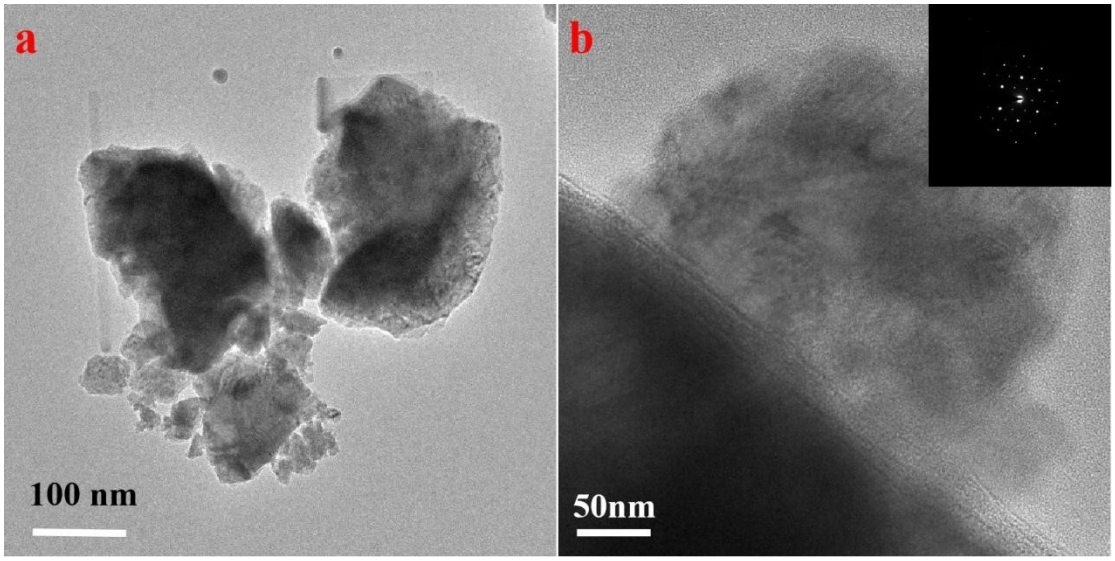

Fig. S4. TEM images of Ti_6O_{11} support.

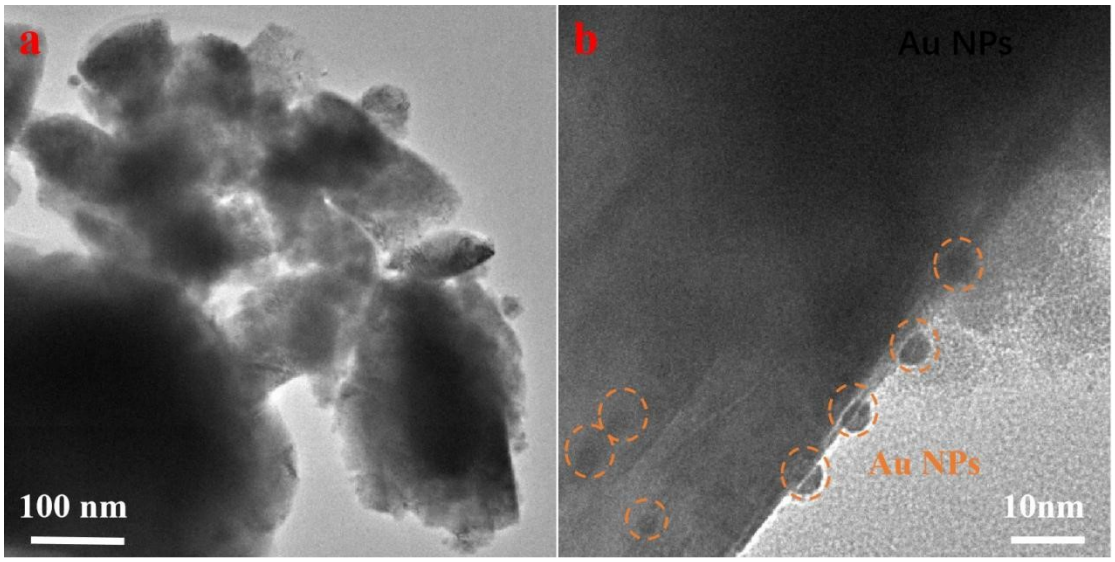

Fig. S5. TEM images of Au (111)@Ti_6O_{11}-50.

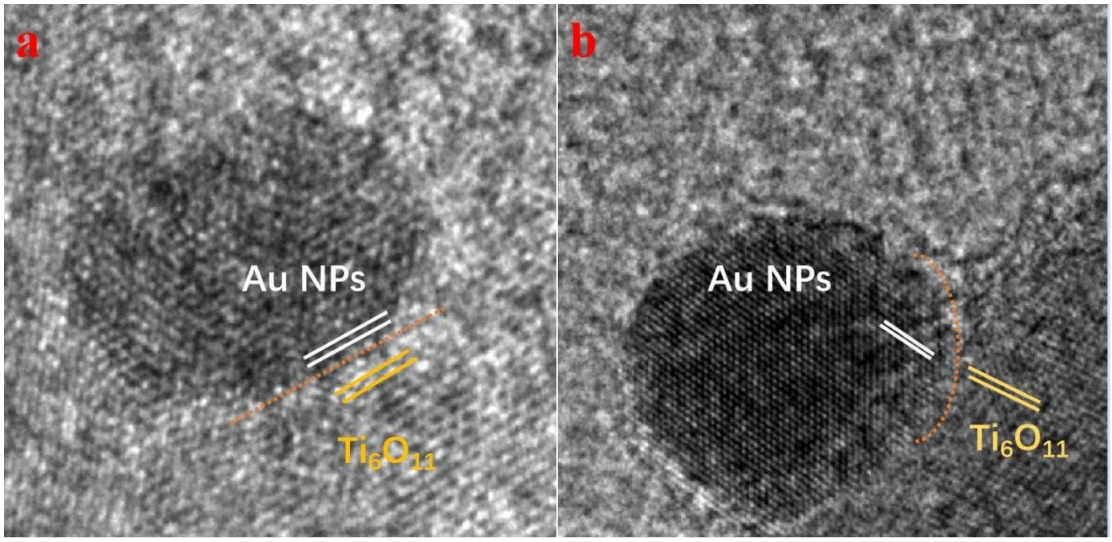

Fig. S6. HRTEM images of Au (111)@Ti_6O_{11}-50.

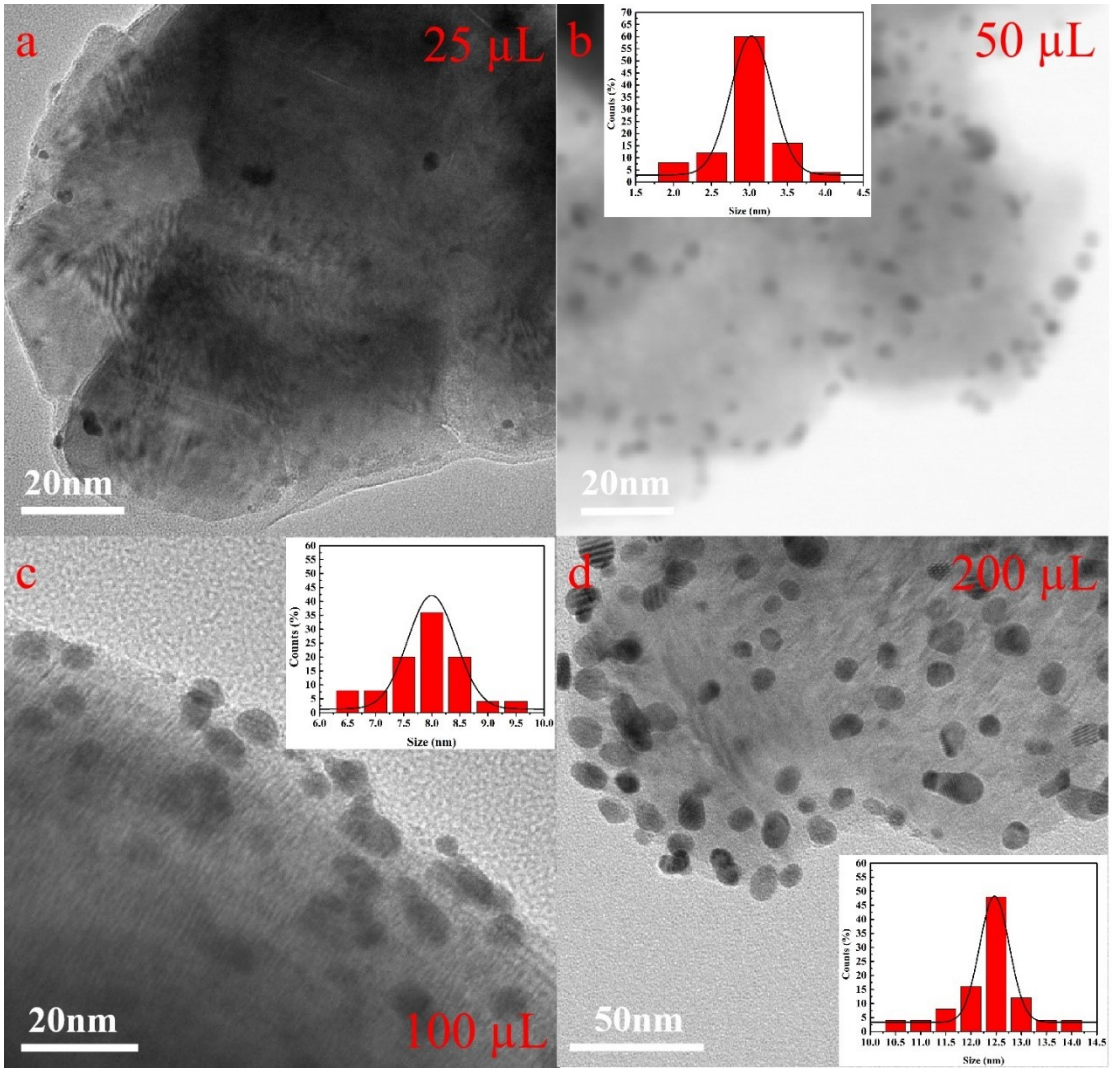

Fig. S7. (a)~(d) The TEM images of Au (111)@Ti_6O_{11}-x, (x=25, 50, 100, 200 μL) (inset：the corresponding size distribution of Au NPs).

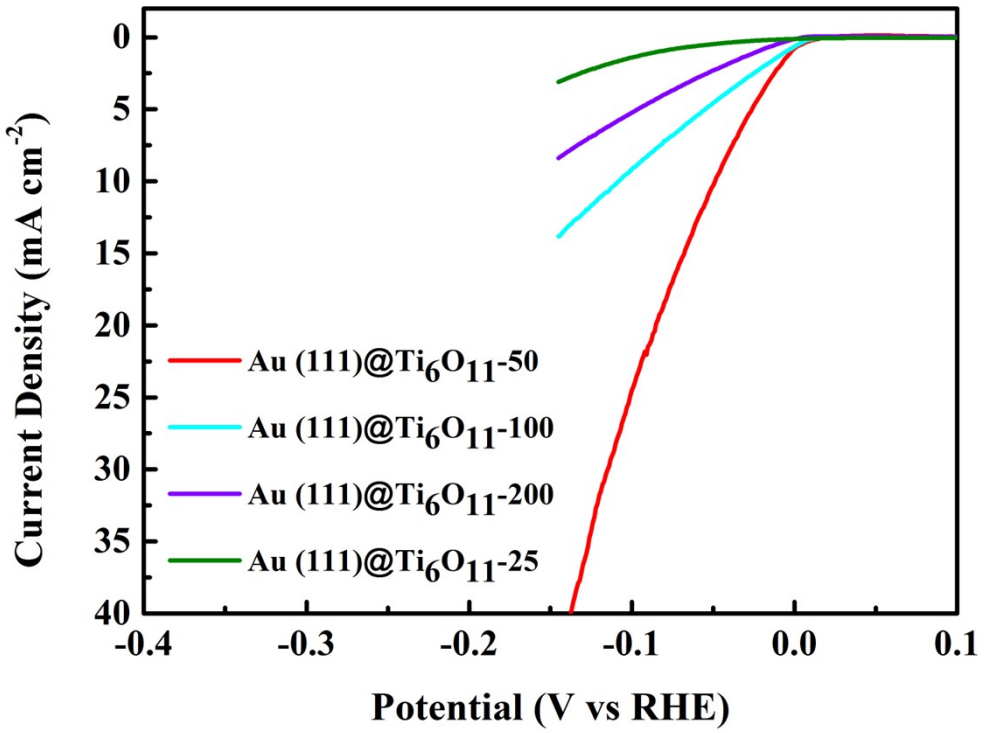

Fig. S8. The LSV curves of Au (111)@Ti_6O_{11}-x, (x=25, 50, 100, 200 μL).

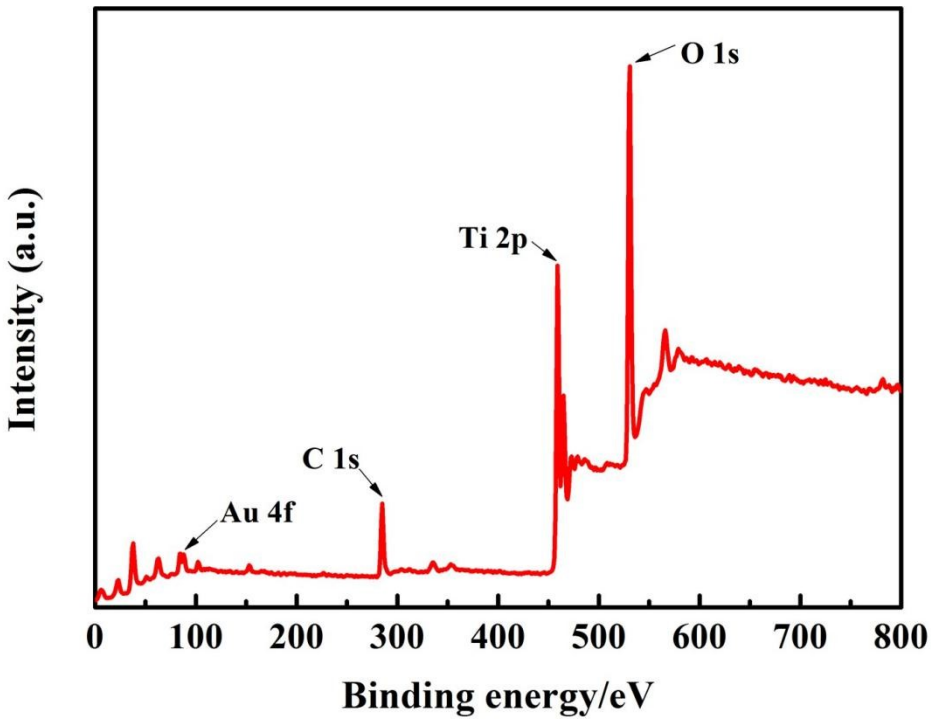

Fig. S9. XPS full spectrum of the Au (111)@Ti_6O_{11}-50.

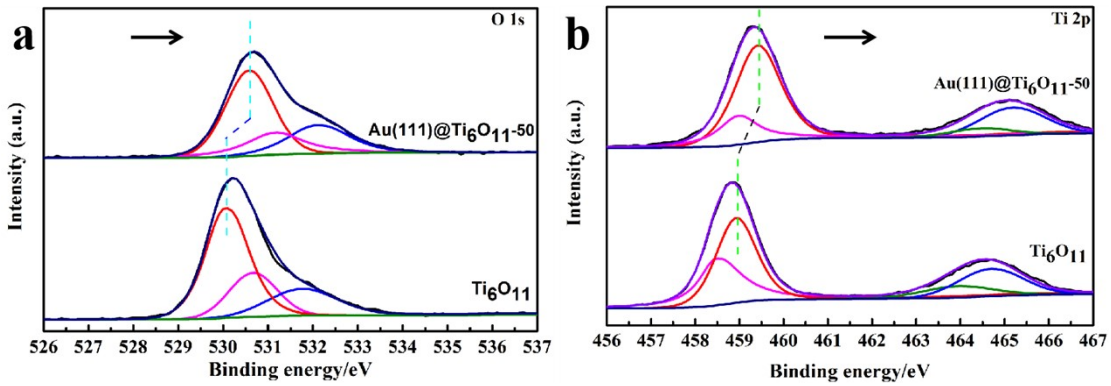

Fig. S10. (a) High-resolution XPS of Au (111)@Ti_6O_{11}-50 and Ti_6O_{11}: O 1s; (b) High-resolution XPS of Au (111)@Ti_6O_{11}-50, Ti_6O_{11}: Ti 2p.

Table S1. The XPS result for Ti 2p

Sample	Peak Position	Peak area	Ti^{3+}/Ti^{4+}
Ti_6O_{11}	Ti^{3+} (458.56)	14813.00	0.365
	Ti^{3+} (464.06)	3503.93	
	Ti^{4+} (459.02)	36148.69	
	Ti^{4+} (464.72)	14044.22	
Au (111)@Ti_6O_{11}-50	Ti^{3+} (458.96)	9446.58	0.290
	Ti^{3+} (464.46)	3746.98	
	Ti^{4+} (459.42)	34684.82	
	Ti^{4+} (465.12)	10805.01	

Table S2. The XPS result for O 1s

Sample	Peak Position	Peak area	V_O/Ti-O
Ti_6O_{11}	Ti-O (530.15)	39479.59	0.414
	V_O (530.75)	16340.57	
	O-H (531.85)	18874.23	
Au (111)@Ti_6O_{11}-50	Ti-O (530.5)	33424.75	0.379
	V_O (531.1)	12685.72	
	O-H (532.05)	16167.29	

Table S3. Comparison of HER performance in acidic media for Au (111)@Ti_6O_{11} with other HER electrocatalysts.

Catalysts	Electrolytes (pH)	□10 (mV) in the media	Tafel slope (mV dec-1)	Mass loading (mg cm^{-2})	Ref.
Au (111)@Ti_6O_{11}-50	0.5 M H_2SO_4	49	39	0.53	This work
Au/Ti_6O_{11}	0.5 M H_2SO_4	138	97.6	0.53	This work
NiCoP/CoP−Ti_4O_7	0.5 M H_2SO_4	128	65.5	0.199	[6]
w-Au@MoS_2	0.5 M H_2SO_4	120	52.9	~	[7]
Au@NC	0.5 M H_2SO_4	130	76.8	0.357	[8]
Mo_2C@NC	0.5 M H_2SO_4	124	60	0.28	[9]
$Mo_{0.25}Co_{0.75}P$/CC	0.5 M H_2SO_4	59	52	~	[10]
MoP@NPSC	0.5 M H_2SO_4	71	75	2.5	[11]
PdNi NWs	0.5 M H_2SO_4	91	98	~	[12]
Ru@WNO-C	0.5 M H_2SO_4	172	38.9	0.357	[13]
Rh-MoS_2	0.5 M H_2SO_4	67	54	0.5	[14]
Pt@MoS_2	0.5 M H_2SO_4	88.43	55.69	~	[15]

CoS2/CoSe2	0.5 M H_2SO_4	80	34	0.285	[16]
FeP/C	0.5 M H_2SO_4	71	52	0.44	[17]
Co/NC	0.5 M H_2SO_4	82	38	0.283	[18]
Fe@FeP/CNT	0.5 M H_2SO_4	53	55	1.6	[19]
$NiSe_2/MoS_2$	0.5 M H_2SO_4	143	45	0.237	[20]
Ru^0/CeO_2	0.5 M H_2SO_4	47	41	0.197	[21]
$MoS_2/Ti_3C_2T_x$	0.5 M H_2SO_4	152	70	0.283	[22]
3-D CNF@CoP/NC	0.5 M H_2SO_4	64.5	48.6	0.5	[23]
RuNi/CFC	0.5 M H_2SO_4	80.2	82.2	0.77	[24]
Mo-MX/C/P	0.5 M H_2SO_4	54	34	0.25	[25]

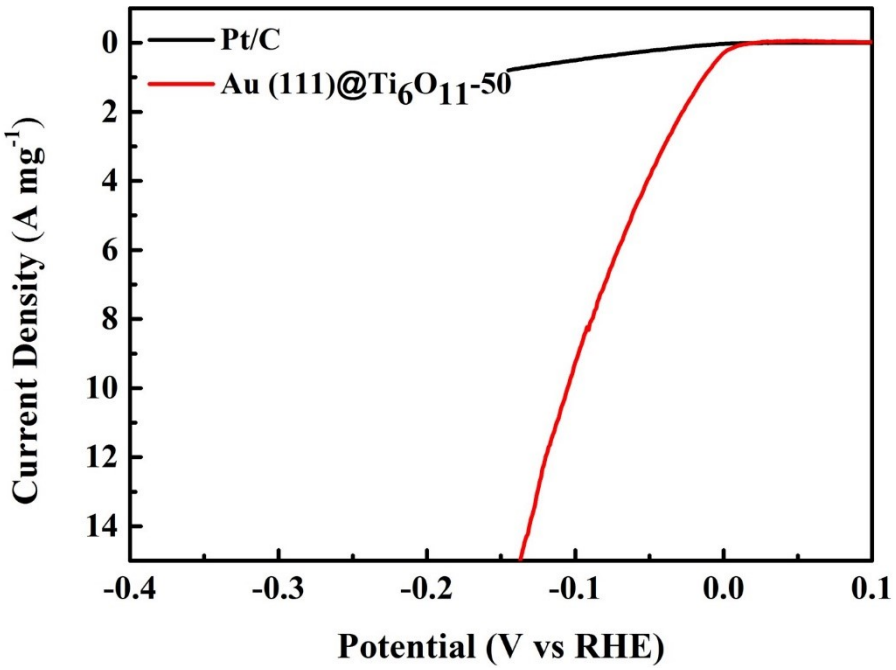

Fig. S11. The polarization curves after normalization for Au (111)@Ti_6O_{11}-50 and Pt/C.

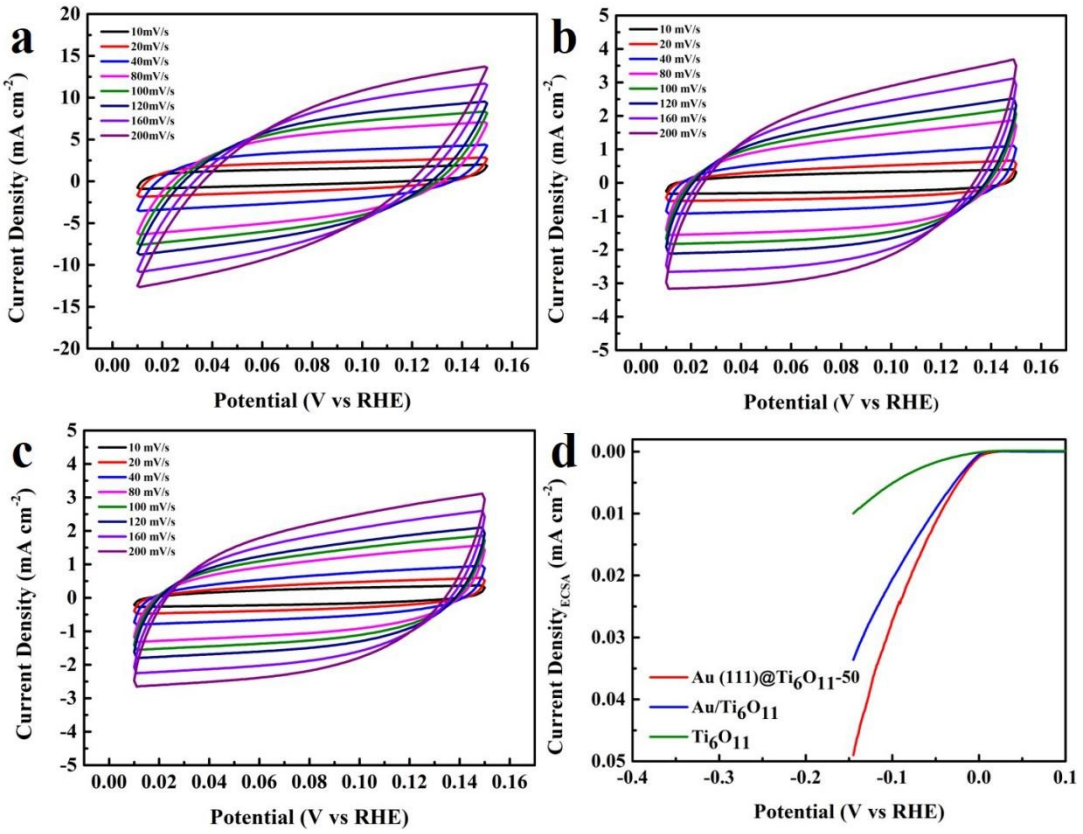

Fig. S12. (a)(b)(c) Typical cyclic voltammetry curves of Au (111)@Ti_6O_{11}-50, Au/Ti_6O_{11} and Ti_6O_{11} with different scan rates from 10 to 200 mV s^{-1} in the potential range of 0.01-0.15 V. (b) Capacitive current at 0.08 V based on scan rate for Au (111)@Ti_6O_{11}-50, Au/Ti_6O_{11} and Ti_6O_{11} ($\Delta j_0 = (j_a - j_c)/2$); (d) Polarization curves normalized by ECSA for these electrocatalysts recorded in 0.5 M H_2SO_4 at a scan rate of 5 mV s^{-1}.

Table S4. Comparison of the Capacitance (C) and ECSA of HER electrocatalysts.

Electrocatalyst	C (mF cm^{-2})	ECSA (cm^2)
Au (111)@Ti_6O_{11}-50	36.03	900.8
Au/Ti_6O_{11}	12.95	323.7
Ti_6O_{11}	9.75	243.7

The electrochemical surface area (ECSA) of catalysts is further estimated by cyclic voltammetry (CV).[26-28] The specific capacitance for a flat surface is generally found to be in the range of 20~60 μF cm^{-2}. 40 μF cm^{-2} is used in the following calculations of the ECSA. The following formula is used to calculate ECSA:

$$\text{ECSA} = \frac{C}{40\ \mu F\ cm^{-2}\ per\ cm^{-2}}$$

Calculation of turnover frequency (TOF)

To calculate the TOF values, we used the previously reported calculation method:[29-32]

$$TOF = \frac{number\ of\ total\ hydrogen\ turnovers / cm^2\ of\ geometric\ area}{number\ of\ active\ sites / cm^2\ of\ geometric\ area}$$

The total number of hydrogen turnovers (No. of H2) was obtained by the following equation:

$$No.of\ H_2 = (j\frac{mA}{cm^2})(\frac{1\,Cs^{-1}}{1000mA})(\frac{1\,mol\ e^{-1}}{96485.3C})(\frac{1\,mol\ H_2}{2\,mol\ e^{-1}})(\frac{6.022*10^{23}\,H_2\ molecules}{1\,mol\ H_2})$$

$$= 3.12*10^{15}\ \frac{H_2/s}{cm^2}\ per\ \frac{mA}{cm^2}$$

The number of active sites (No. of active sites) was estimated as the number of surface sites (Au atoms as the possible active sites). The active sites per real surface area is calculated from the following equation:[31, 33]

$$No.\ of\ active\ sites = (\frac{No.\ of\ atoms / unit\ cell}{volume / unit\ cell})^{\frac{2}{3}}$$

The Au (111)@Ti6O11-50 phase (JCPDS Card No.50-0788), a=14.378, b=9.899, c=35.65 (from DFT results), contains: 80 Au atoms.

$$No.\ of\ active\ sites\ (Au(111)@Ti_6O_{11}-50) = (\frac{80\ atoms / units\ cell}{5073.99\ \overset{o}{A}^3 / unit\ cell})\frac{2}{3} = 0.63*10^{15}\ atoms\ cm^{-2}$$

Finally, the current density can be converted into a TOF according to the following formula:[30]

$$TOF = \frac{(3.12*10^{15}\ \frac{H_2/s}{cm^2}\ per\ \frac{mA}{cm^2})*|J|}{No.\ of\ active\ sites * ECSA}$$

In this work, we calculated the TOF of Au at η =100 mV:

$$TOF_{Au} = \frac{(3.12*10^{15}\ \frac{H_2/s}{cm^2}\ per\ \frac{mA}{cm^2})*|J|}{0.63*10^{15}\ atoms\ cm^{-2}*900.8\,cm^2} = 0.135\ s^{-1}\ atom^{-1}$$

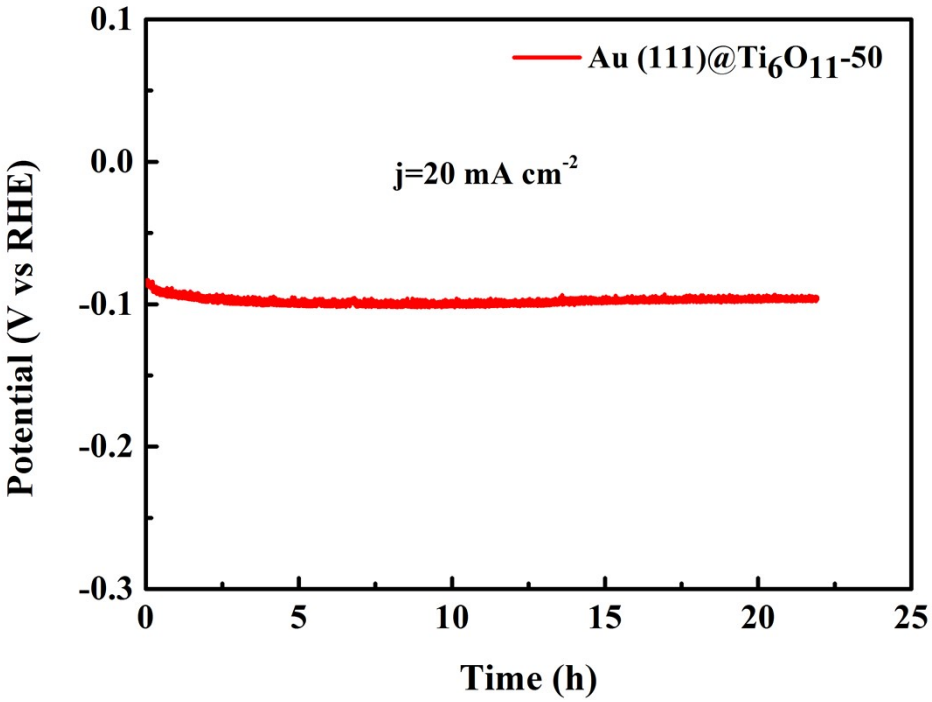

Fig. S13. Chronopotentiometry curve at 20 mA cm^{-2} for the Au (111)@Ti_6O_{11}-50.

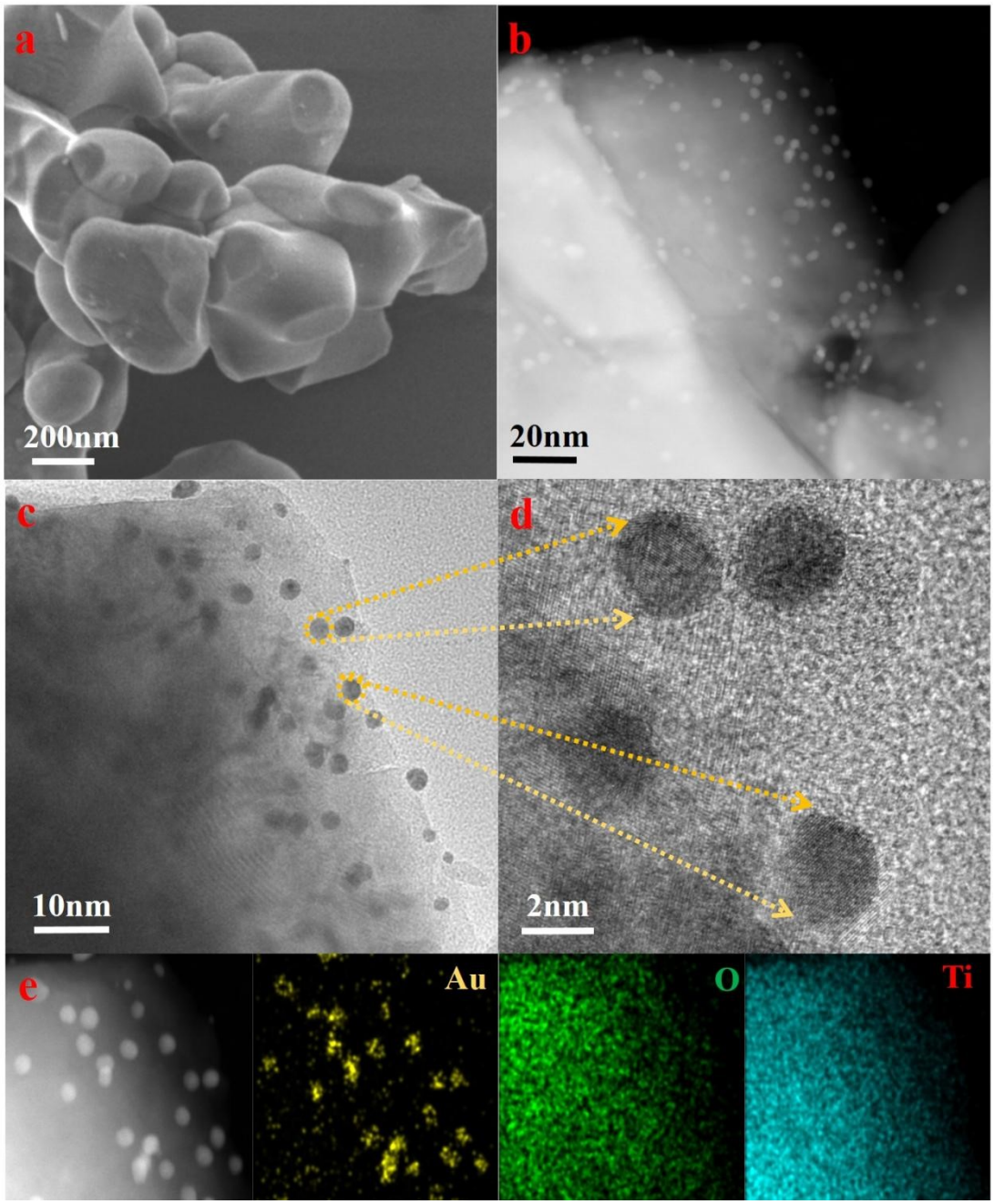

Fig. S14. (a) SEM, (b) high-angle annular dark-field (HAADF)-STEM, (c) TEM, (d) HRTEM images and (e) EDS element mapping images of Ti, Au and O of Au/Ti_6O_{11} after the stability test.

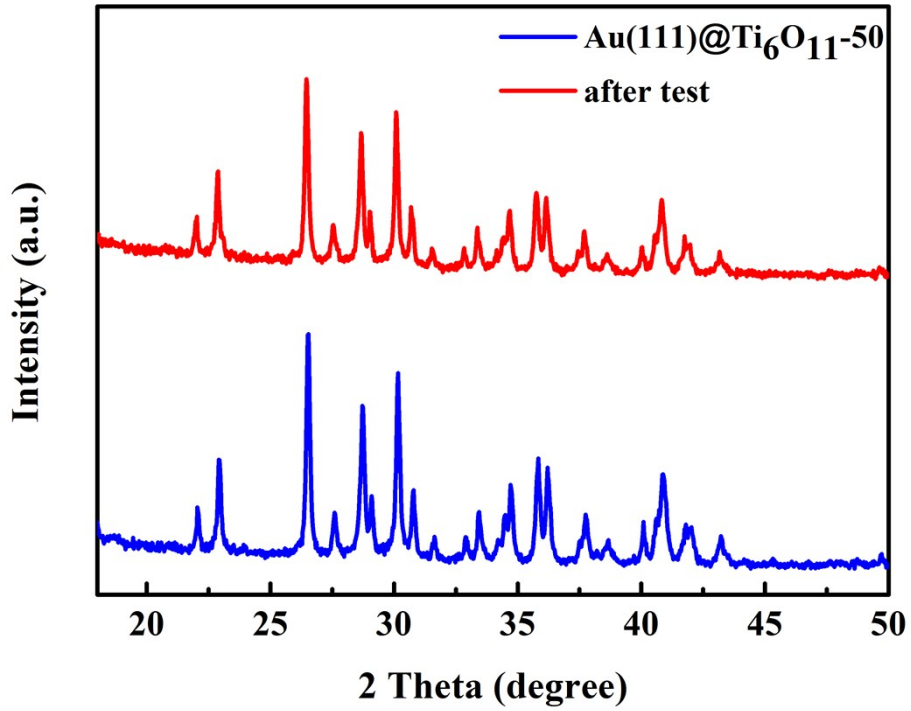

Fig. S15. XRD patterns of the Au (111)@Ti_6O_{11}-50 before and after long-time test.

References

1. J. Perdew, K. Burke and M. Ernzerhof, Phys. Rev. Lett., 1996, 77, 3865-3868.
2. G. Kresse, Phys. Rev. B: Condens. Matter, 1999, 59, 1758-1775.
3. X. Xie, Y. Li, Z.-Q. Liu, M. Haruta and W. Shen, Nature, 2009, 458, 746-749.
4. X. Gu, J.-l. Liu, J.-h. Yang, H.-j. Xiang, X.-g. Gong and Y.-y. Xia, J. Phys. Chem. C., 2011, 115, 12672-12676.
5. A. Galyamova, K. Shin, G. Henkelman and R. M. Crooks, J. Phys. Chem. C., 2020, 124, 10045-10056.
6. D. Ma, R. Li, Z. Zheng, Z. Jia, K. Meng, Y. Wang, G. Zhu, H. Zhang and T. Qi, ACS Sustainable Chem. Eng., 2018, 6, 14275-14282.
7. Y. Li, M. B. Majewski, S. M. Islam, S. Hao, A. A. Murthy, J. G. DiStefano, E. D. Hanson, Y. Xu, C. Wolverton, M. G. Kanatzidis, M. R. Wasielewski, X. Chen and V. P. Dravid, Nano Lett., 2018, 18, 7104-7110.
8. W. Zhou, T. Xiong, C. Shi, J. Zhou, K. Zhou, N. Zhu, L. Li, Z. Tang and S. Chen, Angew. Chem. Int. Ed. Engl., 2016, 55, 8416-8420.
9. Y. Liu, G. Yu, G. D. Li, Y. Sun, T. Asefa, W. Chen and X. Zou, Angew. Chem. Int. Ed. Engl., 2015, 54, 10752-10757.
10. Y. Zhang, Z. Wang, F. Du, H. He, A. Alsaedi, T. Hayat, T. Li, G.-L. Li, Y. Zhou and Z. Zou, J. Mater. Chem. A, 2019, 7, 14842-14848.
11. Y. Jiao, H. Yan, R. Wang, X. Wang, X. Zhang, A. Wu, C. Tian, B. Jiang and H. Fu, ACS Appl. Mater. Interfaces, 2020, 12, 49596-49606.
12. L. Du, D. Feng, X. Xing, C. Wang, G. S. Armatas and D. Yang, Chem. Eng. J., 2020, 400.
13. G. Meng, H. Tian, L. Peng, Z. Ma, Y. Chen, C. Chen, Z. Chang, X. Cui and J. Shi, Nano Energy, 2021, 80.
14. X. Meng, C. Ma, L. Jiang, R. Si, X. Meng, Y. Tu, L. Yu, X. Bao and D. Deng, Angew. Chem. Int. Ed. Engl., 2020, 59, 10502-10507.
15. Y. Li, Q. Gu, B. Johannessen, Z. Zheng, C. Li, Y. Luo, Z. Zhang, Q. Zhang, H. Fan, W. Luo, B. Liu, S. Dou and H. Liu, Nano Energy, 2021, 84.
16. Y. Guo, C. Shang and E. Wang, J. Mater. Chem. A, 2017, 5, 2504-2507.
17. D. Y. Chung, S. W. Jun, G. Yoon, H. Kim, J. M. Yoo, K. S. Lee, T. Kim, H. Shin, A. K. Sinha, S. G. Kwon, K. Kang, T. Hyeon and Y. E. Sung, J. Am. Chem. Soc., 2017, 139, 6669-6674.
18. Q. Mo, N. Chen, M. Deng, L. Yang and Q. Gao, ACS Appl. Mater. Interfaces, 2017, 9, 37721-37730.
19. X. Li, W. Liu, M. Zhang, Y. Zhong, Z. Weng, Y. Mi, Y. Zhou, M. Li, J. J. Cha, Z. Tang, H. Jiang, X. Li and H. Wang, Nano Lett., 2017, 17, 2057-2063.
20. Y. Huang, J. Lv, J. Huang, K. Xu and L. Liu, Nanotechnology, 2021, 32, 175602.
21. E. Demir, S. Akbayrak, A. M. Onal and S. Ozkar, ACS Appl. Mater. Interfaces, 2018, 10, 6299-6308.
22. J. Liu, Y. Liu, D. Xu, Y. Zhu, W. Peng, Y. Li, F. Zhang and X. Fan, Appl. Catal., B, 2019, 241, 89-94.
23. X. Wang, Y. Fei, W. Zhao, Y. Sun and F. Dong, Nanoscale, 2021, 13, 14705-14712.
24. M. Yuan, C. Wang, Y. Wang, Y. Wang, X. Wang and Y. Du, Nanoscale, 2021, 13, 13042-13047.
25. A. Panda and H. Kim, Nanoscale, 2021, 13, 14795-14806.

26. Y. Yang, K. Zhang, H. Lin, X. Li, H. C. Chan, L. Yang and Q. Gao, ACS Catalysis, 2017, 7, 2357-2366.
27. X.-D. Wang, Y.-F. Xu, H.-S. Rao, W.-J. Xu, H.-Y. Chen, W.-X. Zhang, D.-B. Kuang and C.-Y. Su, Energy Environ. Sci., 2016, 9, 1468-1475.
28. C. Tang, W. Wang, A. Sun, C. Qi, D. Zhang, Z. Wu and D. Wang, ACS Catalysis, 2015, 5, 6956-6963.
29. Z. Chen, D. Cummins, B. N. Reinecke, E. Clark, M. K. Sunkara and T. F. Jaramillo, Nano Lett., 2011, 11, 4168-4175.
30. R. Zhang, X. Wang, S. Yu, T. Wen, X. Zhu, F. Yang, X. Sun, X. Wang and W. Hu, Adv. Mater., 2017, 29, 1605502.
31. E. J. Popczun, J. R. McKone, C. G. Read, A. J. Biacchi, A. M. Wiltrout, N. S. Lewis and R. E. Schaak, J. Am. Chem. Soc., 2013, 135, 9267-9270.
32. H.-W. Liang, S. Brüller, R. Dong, J. Zhang, X. Feng and K. Müllen, Nat Commun, 2015, 6, 1-8.
33. A. Laursen, K. Patraju, M. Whitaker, M. Retuerto, T. Sarkar, N. Yao, K. Ramanujachary, M. Greenblatt and G. Dismukes, Energy Environ. Sci., 2015, 8, 1027-1034.